International Journal of Mechanical and Production Engineering Research and Development (IJMPERD)
ISSN (P): 2249-6890; ISSN (E): 2249-8001
Vol. 7, Issue 6, Dec 2017, 305-312

CORROSION BEHAVIOUR OF Mg-Zr ALLOY IN STIMULATED BODY FLUID

T. JUDSON DURAI[1], M. SIVAPRAGASH[2] & M. EDWIN SAHAYARAJ[3]

[1]*Assistant Professor, Department of Mechanical Engineering, Noorul Islam University, Kumaracoil, Kanyakumari, Tamil Nadu, India*

[2]*Dean, Department of Mechanical Engineering, V. V. College of Engineering, Thisayanvilai, Thirunelveli, Tamil Nadu, India*

[3]*Associate Professor, Department of Automobile Engineering, Noorul Islam University, Kumaracoil, Kanyakumari, Tamil Nadu, India*

ABSTRACT

The Mg-Zr alloy is prepared through powder metallurgy method. The corrosion behavior of Mg-Zr alloy, with various sintering temperature, in stimulated body fluid was studied at 37℃, using immersion and electrochemical corrosion tests. The application of this study is the human body bone implants. The characterization of the alloy was carried out through optical microscopy, XRD (X-ray diffraction) and SEM (scanning electron microcopy). The obtained values reveal that, the crystallite sizes reduce by the increasing sintering temperatures and at the same time, the corrosion rates decrease significantly.

KEYWORDS: Magnesium Alloy, Corrosion, Bio-Medical, Bone Implants & Stimulated Body Fluid

Received: Oct 10, 2017; **Accepted:** Oct 30, 2017; **Published:** Nov 14, 2017; **Paper Id.:** IJMPERDDEC201734

Original Article

INTRODUCTION

The earth's crust has got as its third structural material, Mg (magnesium) with a relative density of 1.74 g/cm^3, apart from aluminum and iron [1]. In areas which require light weight applications like transport and aerospace, magnesium will be the best choice, due to its high strength-to-weight ratio [2]. Materials that are degradable and biocompatible, play an important role of bearing load, because of risk in inflammation by traditional implants like stainless steel. But, absorbable polymer materials are currently used, due to unsatisfactory mechanical properties, while it is found that, magnesium alloys are some of the attractive candidates because, they are ultra-light [3-6]. Corrosion, leading to fast degradation of body constitution is the main shortcoming, in magnesium implants [7-12]. Hence, improvement in resistance to corrosion is an issue, for magnesium alloys' application as load bearing biodegradable implants. In fact, the body metabolism and biological mechanism involve the presence of magnesium. Magnesium by nature is observed as a biodegradable material in human body and therefore, it is very promising in the biomedical [6, 13].

The human body consists of metallic elements: manganese, nickel, calcium, copper, chromium, iron, magnesium, vanadium, zinc, etc.[14]. The increasing concentration of these body elements, will cause problems in human body. Zirconium is chosen as an alloying element for magnesium. It has proven harmless to human body, favorable to corrosion resistance and grain refinement for magnesium alloy [15, 16]. Zirconium is widely used to produce medical devices and surgical implants, due to its corrosion resistance and chemical properties [15, 16]. Many industries have acclaimed powder metallurgy (PM) as an established process, in manufacturing engineering equipment for many years. High duty alloys, composite materials, refractory metals and porous materials can be

manufactured by this method.

PM is a competitor to some other methods, in a cost effective and large scale production of complicated components. Material improvements can be made in most cases, through this technology [17]. Usually, this technology consists of production of controlled blend in metal powders, by pressing suitable die in the mixture, and heating subsequently compacted powder at controlled atmosphere, along with temperature so as to obtain the required strength and density. PM industries have shown a rapid expansion, because of their advantages like material utilization, cost, energy saving, ease of components and other factors [18]. The bioactivity of bone implants are tested using simulated body fluid (SBF) [19]. In this work, Magnesium – Zirconium (Mg-Zr) alloy is formed through powder metallurgy and its corrosion resistance against SBF is reported.

MATERIALS AND METHODS

Sample Preparation

The powders of Magnesium and Zirconium were bought from MEPCO Metal Powder Company, India. The samples of Mg-Zr alloy were formed, with the chemical composition (in wt %) of 99.5Mg/0.5Zr. The powders are mixed properly, according to their respective weight, at 350 rpm for 1 hr. The mixed powder is used to form a billet of sizes 50mm diameter and 30mm height, using compacting pressure of 690Mpa. The aluminum foil is used to cover the compacted billets, to prevent any reaction with oxygen from the atmosphere and then, the samples are sintered in argon environment at 450˚C, 500˚C, and 550˚C, respectively, for sample A, B and C in a muffle, for 1 hr. The samples are then extruded in argon atmosphere at 350˚C, to form a cylindrical rod of 13mm diameter and 400mm length. The colloidal graphite is used as lubricant, for extrusion at the ratio of 17:1, using 150 ton hydraulic vertical press. The rods are heat-treated for 15 minutes in an argon atmosphere at 260˚C, to relieve their stresses followed by cut to make 10mm diameter and 10mm thickness. The finer grades of emery papers 800, 1000, 1200, 1500 and 2000 are used, for polishing the samples.

SBF Preparation

The SBF concentrated solution is prepared, by mixing the following specification $(CH_2OH)_3CNH_2$(6.057g/l),NaCl(7.996g/l),$CaCl_2$(0.278g/l),KCl(0.224g/l),$MgCl_2 \cdot 6H_2O$(0.305g/l),$NaHCO_3$(0.350g/l),HCl(40mL/l),Na_2SO_4(0.071g/l),$K_2HPO_4 \cdot 3H_2O$(0.228g/l), in distilled water for avoiding precipitation in homogeneously nucleated calcium phosphates, or other phases. The pH of plasma in human blood is in the range of 7.3 to 7.4 at 37˚C. Therefore, the pH value in SBF is maintained as 7.3 to 7.4, by the addition of concentrated HCl [20].

Optical Microscopy

The micro structural characterization study is conducted using MVHD-1000 AP/MP, Shanghoui Dahens Optics and Fine Mechanics Co. Ltd, digital micro hardness tester. The samples are etched with a solution of ethanol, acetone, and hydraulic acid, followed by distilled water.

XRD Studies

The XRD studies are conducted on PAN Analytical MP XRD, Netherland, automated with XPERT-PRO diffractometer to conduct XRD analysis. The CuK_α radiation (λ=1.5406), scanning speed 3.175 deg $min^{-1}$and 0.10^o step size are used, for the analysis of the range of diffraction 0-90^o.

Immersion Test

The weighed samples are separately submerged in 100 ml SBF solution, at a time period of 168 hours. The test is done, by avoiding circulation or agitation and by not disturbing its corrosion system. The solution's temperature is maintained at 37˚C, using incubator. The corroded samples are cleaned chemically, using boiling in 15% Cro_3 + 1% $AgCrO_4$ solution, at minimum of one minute followed by acetone wash. The loss in weight is measured after every experiment and their rate of corrosion is calculated, in mg cm^{-2} day^{-1} using Equation (1). The unit conversion is made using equation (2) [19].

$$R = \frac{(W_b - W_a + B) \times 1000}{A \times t} \quad (1)$$

Where

R=corrosion rate, mg $cm^{-2}day^{-1}$

W_b=weight of the sample before test (g)

W_a=weight of the sample after test (g)

B=weight loss of blank, g (The three clean and unused sample's average weight loss is used as blank correction)

A=surface area of sample, cm^2

t=exposure time, day

$$\text{Corrosion rate (mm } y^{-1}) = \frac{1}{0.274 \times \rho} R \quad (2)$$

ρ =alloy's density

Electrochemical Test

The electrochemical behavior is studied by Electro chemical analyzer CHI-604D, CH Instruments, USA. The samples are encapsulated using epoxy resin, in order to expose a single face. The test is done in three cell electrode configuration. The sample acts as a working electrode, reference electrode as an SCE (saturated calomel electrode) and counter electrode, as the platinum electrode. The cell is placed in water bath, to maintain the temperature of 37° C, using electric heater and the rate of scan is 1 mV s^{-1}. The corrosion rate is calculated using Equation (3) [19].

$$\text{Corrosion rate (mm } y^{-1}) = \frac{3.28M}{n\rho} i_{corr} \quad (3)$$

n =number of electrons freed, by the corrosion reaction.

M=atomic mass

ρ = density of the specimen.

RESULTS AND DISCUSSIONS

The microstructure of Mg-Zr alloys, at 100X magnification is revealed in Figure.1 (A, B, C), for the sintering temperatures 450°C, 500°C and 550°C, respectively. The pores and cavities appear in all these microstructures. The cavities are reduced, by increasing sintering temperatures as shown in Figure 1(A-C). This could be due to the re-crystallization of alloy, to enhance the grain refinement and during extrusion; grains are deformed to fill the cavities

formed during compaction. Coordinated movement that has occurred among the grains, to improve the stretched grains is replaced by equiaxed and re-crystallized grains [21]. The grain deformation phenomenon is evident from a stretched structure, as shown in Figure 2.

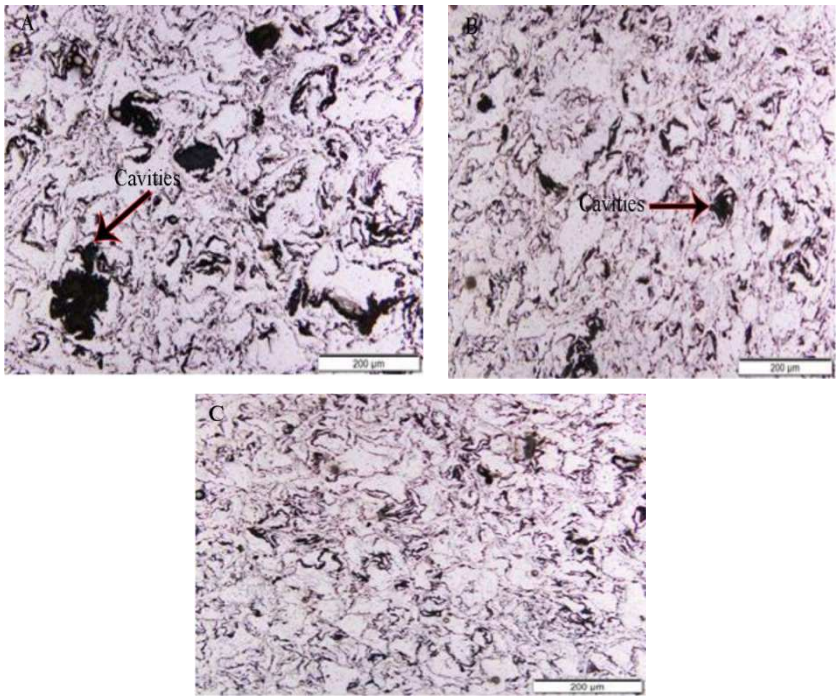

Figure 1: Microstructures of Mg-Zr Alloy of Varying Sintering Temperatures (A) 450°C, (B) 500°C, (C) 550°C

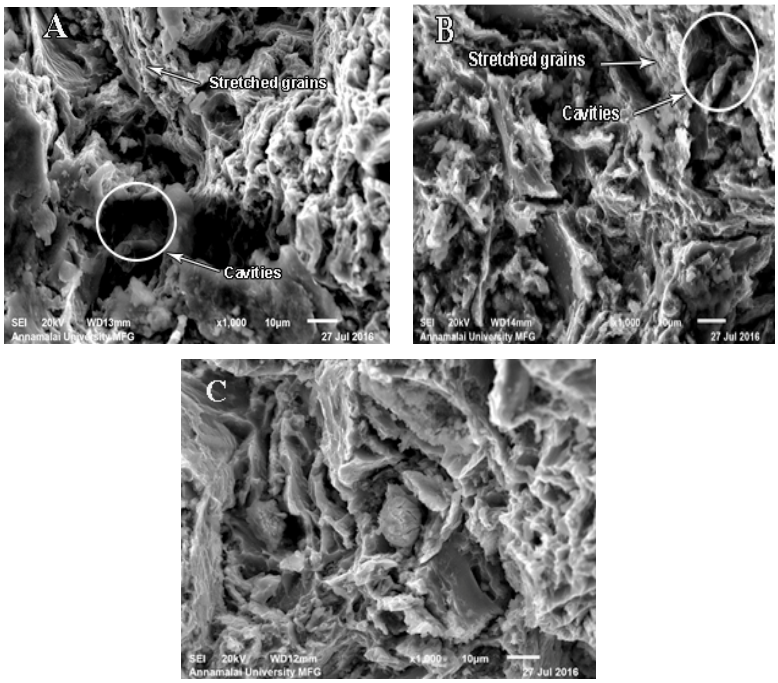

Figure 2: SEM Images of Mg-Zr Alloy of Varying Sintering Temperatures (A) 450°C, (B) 500°C, (C) 550°C

The XRD patterns for the Mg-Zr alloys system, for the sintering temperatures of 450°C, 500°C and 550°C are

depicted in Figure.3. The maximum intensity of magnesium peak appears at 36° [1 0 1], and the zirconium peak appears at 34° [1 1 1], as shown in Figure.3. The diffraction peak angles of Mg and Zr are gradually moved to the right, with increasing sintering temperature. This could be due to the re-crystallization of the alloy constituents. The full width at half maximum of both the phases is also reduced, with increasing sintering temperature. The crystallite sizes of Mg and Zr 32µm and 24µm are used to make an Mg-Zr alloy. The changes in crystallite sizes, after sintering are calculated from the diffraction peaks of magnesium [101] and zirconium [111], as shown in Figure.3, using Debye-scherrer equation [22]. The calculated values of crystallite sizes are depicted in Figure.4.

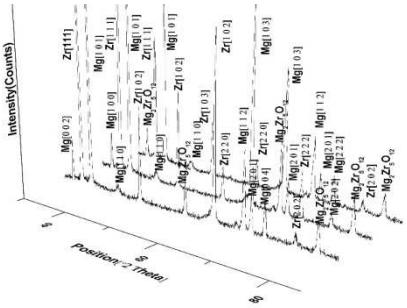

Figure 3: The XRD Patterns of Mg-Zr Alloy for the Sintering Temperatures of 450°C, 500°C and 550°C

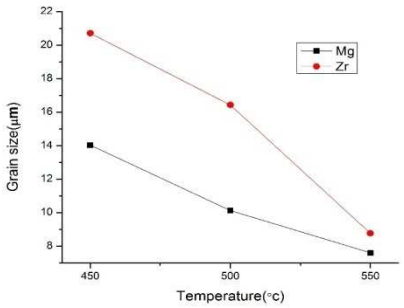

Figure.4 Crystallite Sizes of Mg-Zr Alloy with varying Temperature

The increasing sintering temperature refines the grains of both Mg and Zr, as shown in Figure.4. The very fine grains of Mg are obtained at the sintering temperature, 550°C. This temperature is closer to the melting temperature of Mg of 650°C. Therefore, the grain deformation might be terminated and the formed finer grains fill the cavities. There are not much grain size changes that occur in Zr, during the sintering temperature range 500°C. A drastic drop in grain size of Zr is obtained after 500°C. Moreover, at this 550°C temperature, both the Mg and Zr grain sizes are almost equal. Therefore, the homogeneity of the alloy system improves, so as to reduce the porosity. The reduction in cavity and porosity enhances the corrosion resistance of the alloy [23].

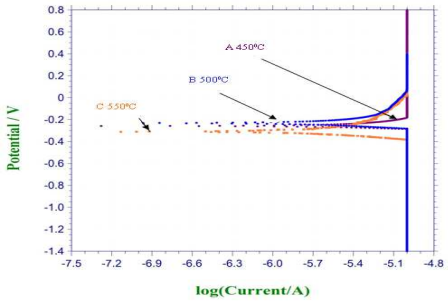

Figure 5: Electrochemical Corrosion Behavior of Mg-Zr Alloy

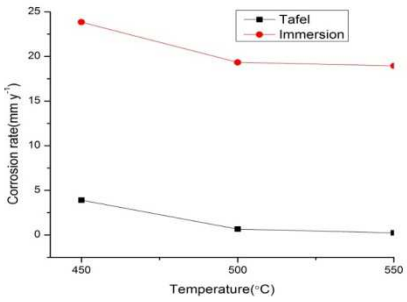

Figure 6: Corrosion Rate of Mg-Zr Alloy with Varying Temperature

The polarization behavior of the specimens in SBF is shown in Figure 5, and the corrosion current I_{corr} is obtained from this plot. The immersion and electrochemical corrosion rate are depicted in Figure 6. The results show that, sample A had the maximum corrosion rate over the other samples (B&C), for both the tests. This could be due to the presence of higher cavities, as mentioned earlier. In general, when the sample is exposed to the SBF solution, the corrosion reaction is carried out through outer surface layer, into the inner layer. In contrast, in the presence of cavities, SBF might enter the cavities, during exposure and get accumulated in it. The accumulated SBF could react with the inner layers of the sample,

which increases the corrosion reaction, unlike the normal corrosion, which takes place in the samples through outer layer into inner layer. Therefore, sample A has higher corrosion rate than the other samples B&C. The increasing sintering temperature decreases the cavities, which in turn, decreases the corrosion rate.

When comparing the samples B&C, the corrosion rates are almost constant for both the samples. This could be due to the corrosion reaction of SBF solution, formed during the new phase of $Mg_2Zr_5O_{12}$ precipitates. This precipitates fill the pores and cavities, present in the surface of the sample, which reduces the rate of reaction on the samples. When comparing all the samples, sample A has more cavities; therefore, this effect could be negligible, unlike the other samples. The obtained corrosion potential (E_{corr}) and current density (i_{corr}) values, for all polarization curves are summarized in Table 1. The E_{corr} values of increasing sintering temperature are shifted to negative side, showing more cathodic behavior of the samples, and the corrosion currents decrease, accordingly. The element Zr has strong chemical affinity with oxygen, to form zirconium oxide layer. The formation of a Zirconium oxide layer can hinder the charge transfer process during corrosion and therefore, decreasing corrosion rate occurs. The wt% of Zr added in this alloys is less as 0.75%, therefore its effect of corrosion rate is less, as compared to the huge quantity of magnesium. However, it produces galvanic corrosion.

Table 1: Electrochemical Behavior of Mg-Zr Alloy

Specimen	Temperature/˚C	Corrosion Potential, E_{corr}(mV)	Corrosion Current Density, i_{corr} (mA/cm^2)
Mg/0.5wt% Zr	450˚C	-0.134	0.2007
Mg/0.5wt% Zr	500˚C	-0.232	0.0339
Mg/0.5wt% Zr	550˚C	-0.310	0.0118

During corrosion, the Co_3^{2-}, $Po_4^{3-}$and Cl^- ions are separated from the SBF solution and the chemical reaction with the specimen surface causes accumulation of OH^- ion, on the specimen surface that is essential for the nucleation of apatite. The faster degradation of magnesium, during the initial implantation stage could affect the surrounding tissue response. Moreover, this could cause rapid osteolysis, which adversely affects the regeneration of bone tissue [24]. The increasing time increases the accumulation of OH^- ions and dissolves the magnesium ions rapidly. The Mg-Zr alloy, with the sintering temperature range 500°C-550°C, causes much more change in corrosion rate, and the formation of $Mg_2Zr_5O_{12}$ precipitates withstands the initial degradation of Mg. Therefore, this could be benefited for the growing of tissues, surrounded by the implants.

CONCLUSIONS

- The Mg –Zralloy is developed by powder metallurgy process, followed by hot extrusion.
- The micro structural studies manifest pores and cavities in all the microstructures.
- The increasing sintering temperature refines the crystallite size and deforms it to fill the cavities.
- The formation of zirconium oxide hinders the charge transfer process, and thus reduces the corrosion rate.
- The increasing sintering temperature reduces the corrosion rate.
- The corrosion rate could be almost constant between the sintering temperatures, 500°C and 550°C

REFERENCES

1. *Makar GL, Kruger J. Int Mater Rev 1993,38(3),138–43.*
2. *Song GL, Atrens A. AdvEngMater 1999, 1(1), 11-33.*
3. *Kojima Y. Mater. Sci. Forum 2003, 350-3, 3-17.*
4. *Heublein B, Rohde R,KaeseV,NiemeyerM,Hartung W, Haverich A. Heart 2003, 89, 651-656.*
5. *King JF. MaterSciTechnol 2007, 23, 1-14.*
6. *Staiger MP, Pietak AM, Huadmai J, Dias JG. Biomaterials 2006, 9, 1728-1734*
7. *Levesque J, Dube D, Fiset M, Mantovani D. Mater. Sci. Forum 2003, 426–4, 521–526.*
8. *Xin YC, Liu CL, Zhang XM, Tang GY, Tian XB, Chu PK. J. Mater. Res 2007, 22, 2004–2011.*
9. *Witte F, Kaese V, Haferkamp H, Switzer E, Meyer-Lindenberg A, Wirth CJ, Windhagen H. Biomaterials 2005, 17 3557–3563.*
10. *Witte F, Fischer J, Nellesen J, Crostack HA, Kaese V, Pisch A, Beckmann F, Windhagen H. Biomaterials 2006, 7, 1013–1018.*
11. *Xu LP, Yu GN, Zhang E, Pan F, Yang K. J. Biomed. Mater. Res 2007, A 83A, 703–711.*
12. *Liu CL, Xin YC, Tian XB, Chu PK. J. Mater. Res 2007, 22, 1806–1814.*
13. *Song GL, Song SZ. AdvEngMater 2007, 9(4), 298–302.*
14. *Yizao Wan, GuangyaoXiong, HonglinLuo, Fang He, Yuan Huang, Xiaoshong Zhou. Materials and Design 2008, 29, 2034-2037.*
15. *Cao P, Qian M, StJohn DH, and Frost MT. Materials Science and Technology 2003, 20, 585–592.*
16. *Song G and StJohn D. Journal of Light Metals 2002, 2, 1–16.*
17. *Selvakumar N, Ganesan P, Radha P, Narayanasamy R, Pandey KS. J Mater Des 2007, 28, 119-30.*
18. *Al-Qureshi HA, Galiotto A, Klein AN. J Mater process Technol 2005, 166, 135-43.*
19. *Muller L, Muller FA, ActaBiomater 2006, 2, 181–189.*
20. *Wei Zhou, TianShen, NaingNaingAung. Corrosion Science 2010, 52, 1035 – 1041.*
21. *ZHAO Zu-de1, CHEN Qiang, YANG Lin, SHU Da-yu, ZHAO Zhi-xiang, Trans. NonferrousMet. Soc. China 2011, 21, 265-271.*
22. *Edwin Sahayaraj M, WinowlinJappesJepas T, Irulappasamy Siva and Murugan Sundaram Senthil Saravanan. Corros. Rev 2014, 32(1-2), 43–49.*
23. *Edwin Sahayaraj M, WinowlinJappes JT, Siva I. Journal of Advanced Microscopy Research 2014, 9, 16-21.*
24. *Guan RG, Johnson I, Cui T, Zhao T, Zhao ZY, Li X, Liu H, J. Biomed Mater Res A 2012, 100, 999-1015*